The Astrophysical Journal, 809:53 (10pp), 2015 August 10 doi:10.1088/0004-637X/809/1/53

PROSPECTS FOR JOINT GRAVITATIONAL WAVE AND SHORT GAMMA-RAY BURST OBSERVATIONS

J. Clark[1,2], H. Evans[1], S. Fairhurst[1], I. W. Harry[1,3], E. Macdonald[1], D. Macleod[1,4], P. J. Sutton[1], and A. R. Williamson[1]
[1] School of Physics and Astronomy, Cardiff University, Cardiff, UK
[2] University of Massachusetts Amherst, Amherst, MA 01003, USA
[3] Department of Physics, Syracuse University, Syracuse, NY, USA
[4] Louisiana State University, Baton Rouge, LA 70803, USA
Received 2014 October 14; accepted 2015 July 6; published 2015 August 10

ABSTRACT

We present a detailed evaluation of the expected rate of joint gravitational-wave (GW) and short gamma-ray burst (GRB) observations over the coming years. We begin by evaluating the improvement in distance sensitivity of the GW search that arises from using the GRB observation to restrict the time and sky location of the source. We argue that this gives a 25% increase in sensitivity when compared to an all-sky, all-time search, corresponding to more than double the number of detectable GW signals associated with GRBs. Using this, we present the expected rate of joint observations with the advanced LIGO and Virgo instruments, taking into account the expected evolution of the GW detector network. We show that in the early advanced GW detector observing runs, from 2015 to 2017, there is only a small chance of a joint observation. However, as the detectors approach their design sensitivities, there is a good chance of joint observations, provided wide field GRB satellites, such as *Fermi* and the Inter planetary Network, continue operation. The rate will also depend critically upon the nature of the progenitor, with neutron star-black hole systems observable to greater distances than double neutron star systems. The relative rate of binary mergers and GRBs will depend upon the jet opening angle of GRBs. Consequently, joint observations, as well as accurate measurement of both the GRB rate and binary merger rates, will allow for an improved estimation of the opening angle of GRBs.

Key words: gamma-ray burst: general – stars: black holes – stars: neutron

1. INTRODUCTION

Two distinct classes of gamma-ray bursts (GRBs) were first proposed by Kouveliotou et al. (1993), who argued for distinct populations of bursts with different durations and spectral hardness. The separation between short and long bursts is typically taken to be a duration of two seconds. Long GRBs have subsequently been associated with the death of massive stars, based on the localization of afterglows to the star forming regions of galaxies (Bloom et al. 1998) and the association of long GRBs with supernovae (Hjorth et al. 2003). Mergers of binary neutron star (BNS) or neutron star-black hole (NSBH) systems are strong candidates for the progenitor of short GRBs (Eichler et al. 1989). There is a large amount of evidence in support of the binary merger progenitor hypothesis (Berger 2014), although nothing definitive.

Binary mergers are also strong emitters of gravitational waves (GW), at frequencies which the LIGO and Virgo detectors have good sensitivity (Thorne 1987). Consequently, it makes sense to search for GW signals originating at a time and sky position consistent with the observed GRB signal. This significantly reduces the size of the GW parameter space by restricting the time, sky location and component masses of the binary (Williamson et al. 2014). An observed signal would allow for the unambiguous identification of a binary merger origin of a short GRB, providing the strongest possible backing for the favored progenitor model. To date, numerous searches for GWs associated with short GRBs (Abadie et al. 2012b; Aasi et al. 2014) have been performed with the data from the initial LIGO and Virgo detectors (Acernese et al. 2007; Abbott et al. 2009). Overall, GW searches have been performed around the time of 80 short GRBs (Aasi et al. 2014), with no evidence of a signal. Given the sensitivity of the detectors (tens of Mpc for BNS and NSBH mergers) and the typical measured redshifts of short GRBs (median $z = 0.4$), this was to be expected. There were, however, two short GRBs, GRB 051103 (Hurley et al. 2010) and GRB070201 (Hurley et al. 2007), whose sky locations overlapped nearby galaxies. The non-detection of GWs associated with these GRBs (Abbott et al. 2008; Abadie et al. 2012a) provided weight to the argument that these events were extra-galactic giant magnetar flares.

The second generation of GW interferometric detectors, Advanced LIGO (Aasi et al. 2015) and Advanced Virgo (Acernese et al. 2015), are under construction and expected to be operational in 2015 and 2016, respectively, approaching design sensitivities over 3–5 years (Aasi et al. 2013). They will provide a factor of ten increase in sensitivity over a broad range of frequencies, and will therefore be sensitive to binary mergers within a few hundred Mpc for BNS and up to 1 Gpc for NSBH (Abadie et al. 2010b), comparable with the distances to the closest short GRBs. The observation of a GW signal in coincidence with a GRB is therefore a realistic prospect. Such an observation would firmly establish binary mergers as the progenitors of short GRBs and also allow us to distinguish a BNS or NSBH progenitor in many cases. This paper discusses in detail the prospects of such a joint observation as the advanced detector network evolves toward its design sensitivity.

In order to accurately evaluate the detection prospects, we must evaluate the expected rates of short GRBs in the local universe and the sensitivity and sky coverage of both the GRB and GW detectors. Numerous studies have provided estimates of the rates of binary mergers and GRBs within the range of the advanced GW detectors (see, for example Abadie et al. 2010b or Wanderman & Piran 2015). Using these, it is possible to estimate the fraction of GRBs that will produce an observable GW signal. In addition to GRB rates and detector sensitivities, this will also depend upon the masses of the progenitors (and in

particular whether they are BNS or NSBH systems) as well as the beaming angle. We obtain an estimate of the rate of joint observations, and show that there is a greatly increased chance of observing a GW around the time of a GRB, in comparison to an arbitrary stretch of data. This increased detection probability allows for a reduction of the detection threshold, to maintain a fixed false detection probability. A timeline for the expected evolution in sensitivity of the advanced LIGO (including LIGO India) and Virgo detectors is given in Aasi et al. (2013). We use this to calculate the expected rate of joint GW–GRB observations as the detectors evolve toward their full sensitivities.

The measure of a GRB redshift provides an additional piece of information, above and beyond the observed time and sky location, that can be used to restrict the parameters of the GW search. This will be valuable as the vast majority of observed GRBs are expected to be outside the range of the GW detectors. By incorporating this information into the GW search, it should be possible to increase the sensitivity of the search to GRBs with measured redshift.

The electromagnetic emission from short GRBs is believed to be be beamed. The jet beaming angle can be measured by observing a jet break in the electromagnetic emission (Sari et al. 1999), and several opening angles have been measured to be less than 10°, with other short GRBs having lower limits up to 20° (Berger 2014). It will be difficult to constrain the opening angle based on the observation of a GW signal, due to the low signal-to-noise ratio of the observations, and an inability to independently measure distance and binary inclination. However, the beaming angle will also affect the relative rates of observed binary mergers and short GRBs: more tightly beamed emission will lead to a lower fraction of binary mergers with observable gamma-ray emission. Consequently, the accurate measurement of both the local GRB rate and the binary merger rate will allow us to infer the (average) beaming angle. Even in the absence of a GW detection, we can place lower bounds on the short GRB jet opening angle. We also present the expected bounds from early advanced detector runs.

This paper is laid out as follows. In Section 2 we discuss GRB observations, briefly reviewing the evidence for the binary merger model of short GRBs and detailing the GRB model we use to obtain our results. In Section 3, we discuss targeted GW searches, providing a brief discussion of previous searches and an evaluation of the sensitivity improvement afforded by a GRB observation. We present the prospects for joint observations in Section 4 and in Section 5 we discuss the benefits of these observations, focusing on redshift measurements and constraining the opening angle. We end, in Section 6, with a discussion.

2. OBSERVATIONS OF SHORT GRBS

2.1. GRB Satellites and Observations

The first GRBs were observed by the Vela satellites (Klebesadel et al. 1973), although it was not until the Burst and Transient Source Explorer instrument on the Compton Gamma Ray Observatory that they were shown to be of cosmological origin, and classified into two families.

GRB observations were revolutionized by the *Swift* satellite which, as well as a large area Burst Alert Telescope (BAT), also carries sensitive X-ray and UV-optical telescopes which can be slewed rapidly to observe the burst afterglow (Gehrels et al. 2004). *Swift* has been operational since 2004, has detected over 800 GRBs to date, including 75 short bursts, and has a field of view of approximately 2 sr. The *Swift* BAT observes around 10 short GRBs per year.[5] It typically gives localizations with arcminute accuracy, or better if the burst is followed up with the onboard X-ray telescope. *Swift*'s ability to localize sources rapidly and accurately has enabled the follow-up observation of numerous short burst afterglows, measurements of redshifts and identification of galaxy hosts. The *Swift* satellite is expected to continue operations until at least 2020.

The *Fermi* satellite was launched in 2008 and carries on board the Gamma-ray Burst Monitor (GBM) and the Large Area Telescope (LAT).[6] It is GBM which provides the broadest sky coverage and is essentially an "all-sky" telescope with a field of view of 9.5 sr (Meegan et al. 2009) *Fermi* GBM typically observes around 45 short bursts per year, of which only a small fraction are seen in LAT. The *Fermi* localization is typically accurate to tens or hundreds of square degrees (von Kienlin et al. 2014), making optical followup of these events challenging. To date, no afterglow from a short GRB observed only by *Fermi* has been observed, and consequently the redshifts of these bursts are not known. *Fermi* is currently operational, with its 10 years funding cycle ending in 2018, though it may continue operations further.

The Space-based multi-band astronomical Variable Objects Monitor (SVOM) satellite[7] is a recently approved Chinese-French mission that is scheduled for launch in 2021 (Basa et al. 2008). SVOM will have a similar sky coverage to *Swift*, and will also carry X-ray, optical and UV telescopes that can be rapidly and automatically slewed to observe afterglows.

Finally, the set of instruments which make up the Inter Planetary Network (IPN),[8] are not dedicated GRB satellites, but instead have GRB monitors on board (Hurley et al. 2003). The majority of satellites in the network are unable to localize the bursts individually but it is possible to localize bursts observed in numerous satellites using triangulation. The sizes and shapes of these error regions vary greatly, depending upon the number of satellites and their locations (more distant satellites greatly improve localization). The IPN provides essentially all sky coverage for GRBs, although, given the sensitivity of the detectors, the GRBs observed tend to be brighter.

There are several key pieces of observational evidence to support the binary merger model for short GRBs. The afterglows of several short GRBs have been observed in both the X-ray (Gehrels et al. 2005) and optical (Hjorth et al. 2005) and consequently localized to galaxies. Despite several low redshift observations, there has been no observation of a supernova associated with any of these events. Additionally, the host galaxies of short GRBs are much more varied than long, with a large fraction of late type galaxies which are not observed as hosts of long GRBs. In the binary merger model, the delay time between formation and merger of the binary can take a wide range of values (Dominik et al. 2012), explaining the range of galaxy types observed as hosts of short GRBs. There is also evidence of "hostless" short GRBs that have been ejected from the galaxy (Fong & Berger 2013) which arise naturally from supernova kicks imparting a velocity to the

[5] http://swift.gsfc.nasa.gov/
[6] http://fermi.gsfc.nasa.gov/
[7] http://www.svom.fr/
[8] http://heasarc.gsfc.nasa.gov/W3Browse/all/ipngrb.html

binary, coupled with the long delay time to merger. The strongest evidence for the merger model is the observation of a kilonova associated with GRB130603B (Berger et al. 2013; Tanvir et al. 2013). Taken together, these observations provide good evidence for the binary merger model for at least a subset of short GRBs. We note, however, that some fraction may still be mis-classified long GRBs (Bromberg et al. 2013) or soft gamma repeaters in nearby galaxies (Abbott et al. 2008; Hurley et al. 2010).

2.2. The Rate of Short GRBs

There have been numerous efforts recently to estimate the rate of short GRBs, based primarily on redshift measurements of GRBs observed by *Swift* (Coward et al. 2012; Siellez et al. 2014; Wanderman & Piran 2015).[9] Here, we follow Wanderman & Piran (2015), who use the observed GRB populations (and measured redshifts in *Swift*) in order to derive a luminosity function for GRBs as well as a local rate density.

The energy spectra of short GRBs is modeled, following Band et al. (1993), as a power-law decay with exponential cutoff at low energy and a steeper power law at higher frequencies. The parameters used in the Band function are $\alpha_{\rm BAND} = -0.5$, $\beta_{\rm BAND} = -2.25$ and $E_{\rm peak} = 800$ keV. For a GRB at a given distance/redshift, the peak photon count in a detector can be related to the peak luminosity in a straightforward way (Regimbau et al. 2015; Wanderman & Piran 2015). The detection threshold is taken to be 2.5 photons $\rm s^{-1}$ in the 15−150 keV band for *Swift* and 2.37 photons $\rm s^{-1}$ in the 50−300 keV band for *Fermi*.

The short GRB luminosity function is taken to be a broken power law, with a logarithmic distribution

$$\phi_o(L) = \begin{cases} \left(\frac{L}{L_\star}\right)^{-\alpha_L} & L < L_\star \\ \left(\frac{L}{L_\star}\right)^{-\beta_L} & L > L_\star \end{cases} \quad (1)$$

where L is the peak luminosity (in the source frame) between 1 keV and 10 MeV, and α_L and β_L give the power-law decay below and above the break at $L_\star$.[10] The other important parameter is the minimum GRB luminosity, which determines the lower cutoff of the luminosity distribution. This is poorly constrained as only nearby low luminosity GRBs would be observable. The minimum luminosity is taken to be $L_{\rm min} = 5 \times 10^{49}$ erg $\rm s^{-1}$.

The parameters α_L, β_L, $L_\star$ are fitted jointly with the short GRB rate. Best fit values are $\alpha_L = 1$, $\beta_L = 2$ and $L_\star = 2 \times 10^{52}$ erg $\rm s^{-1}$, with a local GRB rate of 4.1 $\rm Gpc^{-3}$ $\rm yr^{-1}$. The GRB rate evolves with redshift, peaking at $z \approx 1$.

Other works (Coward et al. 2012; Siellez et al. 2014) take a similar approach to estimating the rate of short GRBs, although the assumptions they make vary. Consequently there is some variation in the rate estimates, but they typically lie in the range $(1\text{–}10) \times 10^{-9}$ $\rm Mpc^{-3}$ $\rm yr^{-1}$ with a median rate around 3×10^{-9} $\rm Mpc^{-3}$ $\rm yr^{-1}$. These rates are somewhat lower than earlier estimates based on a smaller sample of GRBs (Guetta & Piran 2006; Nakar 2007). For the remainder of this work, we make use of the Band function and luminosity distribution parameters of Wanderman & Piran (2015), but allow for a constant rate per comoving volume between 1 and 10 $\rm Gpc^{-3}$ $\rm yr^{-1}$. We do not include any variation of GRB rate with redshift as we found it had little impact on the overall results, due to the limited range of the GW detectors.

Given the evidence for a binary merger progenitor for short GRBs, it is interesting to compare the observed and predicted rates of short GRBs and binary mergers. To do so, we must take into account the beaming of the GRB jet. The evidence for beaming in short GRBs comes primarily from the observation of jet breaks, at which time the material in the jet starts to spread out, leading to a break in the light curve. The observation of such a break can be used to infer the jet's opening angle (Sari et al. 1999). The observation of a jet break in a number of short GRB afterglows (see for example Panaitescu 2006; Guelbenzu et al. 2012; Fong et al. 2014) has been used to infer opening angles between 3° and 8°. In others, the lack of an observed break has been used to set a lower limit on the beaming angle. In many cases this leads to a limit of only a few degrees, however, GRB 050724 had no observed break after 22 days, leading to an inferred opening angle of at least 20°. See Berger (2014) for a summary of observations to date.

The rate of observed short GRBs can be related to the all sky rate of binary mergers through

$$R_{\rm GRB} = f_\gamma \left(1 - \cos\theta_j\right) R_{\rm merger} \quad (2)$$

where θ_j is the average jet opening angle of the gamma-ray emission, and the factor f_γ encodes the fraction of binary mergers which produce a GRB. The rate of neutron star binary (BNS) mergers, inferred from binary pulsar observations and population synthesis modeling, is taken to lie between 1×10^{-5} and 1×10^{-8} $\rm Mpc^{-3}$ $\rm yr^{-1}$ (see Abadie et al. 2010b and references therein). To date, no NSBH systems have been observed as binary pulsars, but the rate can still be predicted through population synthesis, constrained by the observations of BNSs, to be $10^{-6} - 6 \times 10^{-10}$ $\rm Mpc^{-3}$ $\rm yr^{-1}$.

In Figure 1, we compare the observed and predicted rates for short GRBs to those for BNS and NSBH mergers. As has been observed elsewhere (Guetta & Piran 2006), there is a remarkable concordance between the GRB and BNS rates, with the observed beaming angles compatible with the best guess BNS rate, with a lower rate of BNS mergers requiring larger GRB opening angles.[11] For NSBH, the rates are not in such good agreement. A 5° jet angle requires an NSBH rate right at the top of the predicted range; alternatively a lower NSBH rate is consistent with a wider opening angle than has been inferred from observations. Furthermore, it is likely that a a reasonable fraction of NSBH mergers will not produce any electromagnetic emission as the NS will be swallowed whole, leaving no material from which to form an accretion disk and,

[9] A nice summary of recent rate estimates is provided in Table 4 of Wanderman & Piran (2015).

[10] Other papers use a smaller energy band when defining the luminosity, and this has an impact on the value of $L_\star$, although not on the slopes of the power law components.

[11] For this discussion, we have implicitly been assuming that *all* BNS mergers, produce GRBs, i.e., $f_\gamma = 1$ in (2). There are, however, arguments that only a subset of BNS mergers will produce GRBs, for example Giacomazzo et al. (2012).

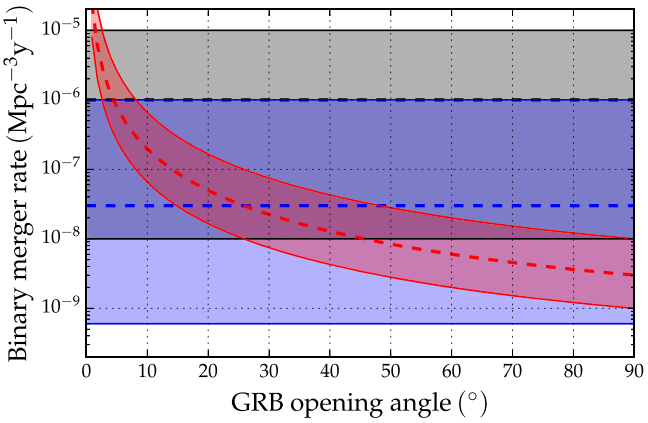

Figure 1. Rate of binary mergers in the local universe. The figure shows the predicted rates of binary neutron star (upper, gray band) and neutron star black hole (lower, blue band) mergers, taken from Abadie et al. (2010b). The shaded regions mark the range of reasonable values, while the dashed lines show the best estimate of the rate. We can also infer the rate of GRB progenitors, given an opening angle, as plotted in red.

hence, GRB jet (Foucart 2012; Pannarale & Ohme 2014). Indeed, in Stone et al. (2013), the fraction, f_γ, of NSBH mergers that produce short GRBs is argued to be between 0.1 and 0.3, depending upon black hole mass and spin distributions. Thus, based on rate estimates, it seems unlikely that NSBH mergers can account for *all* observed short GRBs.

3. GW SEARCHES FOR GRB PROGENITORS

3.1. Implementation of a Targeted Search

The details of the targeted search for GWs associated with short GRBs are presented in Harry & Fairhurst (2011), Williamson et al. (2014). Given the time and sky location of the GRB, the search is restricted to a six second span of data around the GRB, allowing for a merger time 5 s before and 1 s after the time of the GRB. This allows for most realistic delays between the merger and GRB signal. The data from the available GW detectors is combined coherently, by appropriately time shifting and weighting the data from each detector to account for the known sky location of the source, to produce data streams sensitive to the two GW polarizations. The data is then searched through matched filtering using a template bank of binary merger waveforms (Owen & Sathyaprakash 1999; Blanchet 2014). GRBs observed by *Swift* are localized to well under a square degree which, for the GW search means they are effectively localized to a single sky location. For GRBs observed by *Fermi* GBM or the IPN, the sky location may be poorly constrained by satellite observations, with uncertainties of tens to hundreds of square degrees. In this case, a grid of sky points is searched (Predoi & Hurley 2012; Williamson et al. 2014). Additional signal consistency tests (Allen 2005; Harry & Fairhurst 2011), designed to eliminate glitches which have a different signal morphology than binary merger signals, are used to eliminate spurious events due to non-Gaussian noise. The background is evaluated from data surrounding the six second stretch used in the search and simulated signals are added to the data to evaluate the search sensitivity.

3.2. The Benefit of a Targeted Search

The observation of a short GRB provides a good estimate of the merger time, sky location and (possibly) distance of a potential binary merger signal. This significantly reduces the parameter space of a follow-up GW search and consequently allows for a reduction in the detection threshold (Chen & Holz 2013; Dietz et al. 2013; Kelley et al. 2013). We evaluate in detail the sensitivity improvement afforded by the GRB observation. In contrast to most previous studies, we will make use of the results obtained from searches on real data and make use of the results of previous analyses (Abadie et al. 2012c; Williamson et al. 2014).

To investigate the impact of reducing the parameter space for GRB searches, we will deliberately avoid the question of first GW detection—where a "5σ" observation may well be required (Abadie et al. 2012c). Instead, we consider a later observation for which we might require a specific false positive rate: i.e., a limit on the fraction GW observations are spurious. In that case, the threshold for announcing a detection is tied to the true signal rate. Since neither the GRB or BNS rates are known with great accuracy, for this discussion we will adopt with the "realistic" rates of $10^{-6}\,\mathrm{Mpc}^{-3}\,\mathrm{yr}^{-1}$ for BNS mergers and $3\times10^{-9}\,\mathrm{Mpc}^{-3}\,\mathrm{yr}^{-1}$ for short GRBs.

A detailed evaluation of the expected rate of BNS observations is provided in Aasi et al. (2013). There, a false rate of one event per century is chosen, corresponding to a signal-to-noise ratio of 12 in the advanced detectors. When the advanced LIGO and Virgo detectors are operating at design sensitivity, the expected rate of observed BNS mergers is $20\,\mathrm{year}^{-1}$. Thus the threshold corresponds to a false positive rate of 1 in 2000.

To obtain a comparable SNR threshold for the GRB search, we need to evaluate both the expected foreground and background around the time of a short GRB. Using the results of Williamson et al. (2014) we estimate a background rate of 1 in 1000 for event with an SNR above 8 in the GRB search, with the background decreasing by a factor of 100 for a unit increase in SNR:[12]

$$P_{\mathrm{BG}}\left(\rho>\rho_\star\right)=\begin{cases}10^{-\left(5+2\lfloor\rho_\star-9\rfloor\right)} & \rho_\star>6.5\\ 1 & \rho_\star\leqslant 6.5.\end{cases}\qquad(3)$$

Next, we must determine the probability of any given GRB occurring at a low enough redshift that the GW signal would be observable by the advanced LIGO and Virgo network. The sky and binary orientation averaged sensitivity of the network is 200 Mpc. However, it is natural to assume that the GRB jet is beamed perpendicular to the plane of the binary's orbit (see, e.g., Piran et al. 2013). The GW signal is also (weakly) beamed in this direction: the amplitude for a face on signal is a factor of 1.5 greater than the orientation averaged amplitude.[13] The GW beaming is rather weak and the amplitude falls off slowly with

[12] The analysis in Williamson et al. (2014) was performed for the initial LIGO and Virgo detectors and, assuming that GRB emission is beamed and the jet is perpendicular to the plane of the binary, we obtain a background of 1 in 10^5 above SNR of 8. However, we must include a trials factor due to requiring a larger template bank for the advanced detectors (Owen & Sathyaprakash 1999) and consequently we (somewhat conservatively) increase the background by a factor of 100 as was done in Aasi et al. (2013).

[13] The sensitivity of a detector to binary mergers is typically quoted in two different ways: either the range—the sky and orientation averaged sensitivity; or the horizon—the maximal sensitivity, for binaries which are directly overhead the detector and face on. The horizon distance is a factor of 2.26 greater than the range. Here, we are assuming all sources are face on, but still averaging over sky positions. It turns out that the averaging over orientation and sky give the same factor, so performing just one average increases the sensitivity by $\sqrt{2.26}=1.51$.

opening angle. Even with opening angles up to 30° the mean amplitude is only reduced by 5% from the face on case (Dietz et al. 2013). Thus, the nominal sensitivity for GRB signals in the advanced detector network is 300 Mpc, rather than 200 Mpc for signals of arbitrary orientation. The sensitive distance scales inversely with the SNR threshold, i.e.,

$$D_\star = \left(\frac{12}{\rho_\star}\right) 300\ \mathrm{Mpc}. \quad (4)$$

There are around 50 short GRBs observed annually (10 by *Swift* BAT and 45 by *Fermi* GBM, of which several are observed by both instruments). Assuming a local GRB rate of $3 \times 10^{-9}\ \mathrm{Mpc^{-3}\ yr^{-1}}$, we would expect around one event per year to be detected at a distance of 500 Mpc or less, taking into account detector sensitivities, sky coverage and live times. Thus, the chance of any GRB occurring within a distance $D_\star$ can be approximated as

$$P_{\mathrm{GRB}}(D < D_\star) \approx \frac{1}{50}\left(\frac{D_\star}{500\ \mathrm{Mpc}}\right)^3 \quad D_\star \lesssim 500\ \mathrm{Mpc}. \quad (5)$$

We have ignored the impact of detector sensitivity since, assuming the GRB model in the previous section, the majority of GRBs within this range would be observed by *Swift* or *Fermi* if they were in the field of view. This is broadly consistent with the observed redshifts from *Swift*, where the smallest of 30 measurements is $z = 0.12$, corresponding to a distance of 550 Mpc. Obviously, this relationship will break down at larger distances where cosmological effects, variation of the intrinsic GRB rate and detection efficiencies all become significant.

In the GRB search, the chance of a noise event giving an SNR above 9.1 is 5×10^{-6}. At this SNR, the sky averaged sensitivity to face on BNS mergers is 400 Mpc so, from Equation (5), there is a 1% chance of the GW signal from a short GRB being observable. This gives a false positive rate of 1 in 2000 as desired. Therefore, the observation of a GRB allows us to lower the threshold in a GW search by 25% while maintaining a fixed false positive rate. We note that neither the astrophysical rate of BNS or GRBs nor the noise background of the advanced detectors are known at this time. Nonetheless, the predicted increase in sensitivity of the GRB search is relatively robust. The observed background for the BNS and GRB searches is very similar in nature and, in particular, both show the same, rapid rate of falloff at large SNR. Thus, changes in the required detection confidence will affect both searches in the same way.

Reducing the detection threshold by 25% will more than double the number of detectable signals. In other words, less than half of GW signals associated with GRBs will be detected based on the GW signal alone—it is only with a joint search that makes use of the GRB observation that these additional signals will be seen.

It is instructive to ask why the detection threshold can be lowered by 25% for the GRB search. The answer is twofold. First, the expected rate of signals is significantly higher in the data around the time of a GRB. In Equation (5), we gave the probability of there being an observable signal in the six seconds of data around the time of a GRB, as a function of the sensitive distance. Within the nominal GRB range of 300 Mpc (at SNR 12), there is a 1 in 250 chance of observing a signal associated to the GRB. Meanwhile, for an arbitrary six seconds of data, assuming a BNS rate of $10^{-6}\ \mathrm{Mpc^{-3}\ yr^{-1}}$, there is a 1 in 150,000 chance of observing a signal associated to a BNS merger. Thus, assuming that BNS are GRB progenitors, it is around a thousand times more likely that we observe a signal within the six seconds around a GRB than in an arbitrary six seconds of data. In addition, the GRB background is further reduced because searching a small time window makes a fully coherent search feasible (Harry & Fairhurst 2011), and this increases the sensitivity relative to the all sky search (Babak et al. 2013). These factors combine to lead to the 25% reduction in threshold that can be achieved by the search.

4. EXPECTED RATE OF JOINT OBSERVATIONS

The first advanced detector observing runs of the are expected in late 2015, with sensitivity reaching the design specification toward the end of the decade. At design sensitivity, the aLIGO range for BNS mergers will be 200 Mpc and for AdV, 130 Mpc. Around 2022, a third LIGO detector in India is expected to begin observing with comparable sensitivity (Aasi et al. 2013). Given the evolution of the advanced detector sensitivities as well as the results of the previous sections, it is straightforward to evaluate the expectations for joint short GRB–GW observations in the coming years. We consider three GRB observing scenarios: *Swift*, *Fermi*, and full sky, full sensitivity coverage. While the latter is, of course, somewhat optimistic, it serves to provide an upper bound on the joint observation rate. For *Swift* and *Fermi*, we use the sky coverage and detection thresholds outlined in Section 2.1 and, in addition, we assume an 80% detector duty cycle for both detectors due to passage through the South Atlantic Anomaly.

The expected rates of short GRB observations, assuming a BNS progenitor, are given in Table 1. For each observing run, a range of possible detector sensitivities is quoted, to take into account the uncertain nature of commissioning and operating the advanced detectors (Aasi et al. 2013). The rate of observed BNS mergers is calculated for a merger rate between 10^{-5} and $10^{-8}\ \mathrm{Mpc^{-3}\ yr^{-1}}$. The range of predicted rates reflects the uncertainty in both the detector sensitivities and the rate of sources. For joint GW–GRB observations, we take the short GRB rate to lie in the range 10^{-8}–$10^{-9}\ \mathrm{Mpc^{-3}\ yr^{-1}}$. As discussed in Section 3.2, we allow for a 25% decrease in detection threshold associated with a dedicated GRB search when compared to an all-sky all-time GW search. When calculating the *Swift* and *Fermi* rates, we use the GRB luminosity distribution and energy spectra described in Section 2.1. These thresholds, however, have little effect on the rate as the majority of GRBs within the sensitive range of advanced LIGO and Virgo will have a peak luminosity sufficient to be observed by *Swift* BAT and *Fermi* GBM.

The expected number of joint observations in the early advanced LIGO–Virgo science runs is much less than one. However, by the 2017–18 observing run, there is a real chance of a joint observation and, with the network operating at design sensitivity, an excellent chance of joint GW–GRB observations during an extended science run. We note, however, how critical it is to continue monitoring the sky for GRBs: it is only with the sky coverage provided by *Fermi* (and the IPN) that we expect to make joint observations.

Figure 2 shows the expected annual rate of joint observations, as a function of GRB opening angle for the 2019+ configuration of Table 1. The dependence of the rate on the

Table 1
The Expected Rate of Joint Gravitational Wave–GRB Observations in the Upcoming Science Runs, Assuming That the Progenitor of Every Short GRB is a BNS Merger

Epoch	Run Duration	BNS Range (Mpc)		Number of BNS Detections	Number of GW–GRB Detections		
		LIGO	Virgo		All Sky	*Fermi* GBM	*Swift* BAT
2015	3 months	40–80	···	0.0004–3	2×10^{-4}–0.02	2×10^{-4}–0.02	3×10^{-5}–0.003
2016–17	6 months	80–120	20–60	0.006–20	0.004–0.2	0.003–0.1	3×10^{-4}–0.03
2017–18	9 months	120–170	60–85	0.04–100	0.02–0.8	0.01–0.5	7×10^{-4}–0.1
2019+	(per year)	200	65–130	0.2–200	0.1–2	0.07–1	0.01–0.2
2022+	(per year)	200	130	0.4–400	0.2–3	0.1–2	0.02–0.3

Note. Sensitivities, run durations, and BNS rates taken from (Aasi et al. 2013).

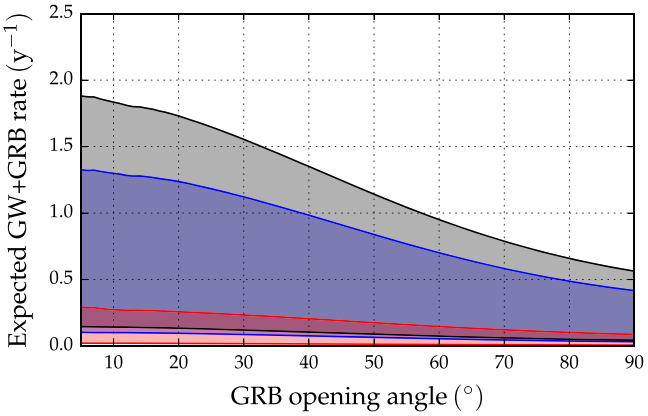

Figure 2. Expected rate of observed gravitational wave–GRB signals when the LIGO and Virgo detectors are operating at their design sensitivity. We take the intrinsic short GRB rate to be in the range $(1\text{–}10) \times 10^{-9}$ Mpc^{-3} yr^{-1} and assume that BNS are the progenitor source of all short GRBs. The gray region shows the range of expected rates with all-sky GRB coverage. The observed rate increases with a small opening angle as the systems are close to face on and thus have the maximum gravitational wave emission. The blue region shows the expected rate for joint observations with *Fermi* GBM and the red region for *Swift* BAT. For preferred opening angles (less than 30°) we expect to see at least one GRB per year in coincidence with *Fermi* GBM.

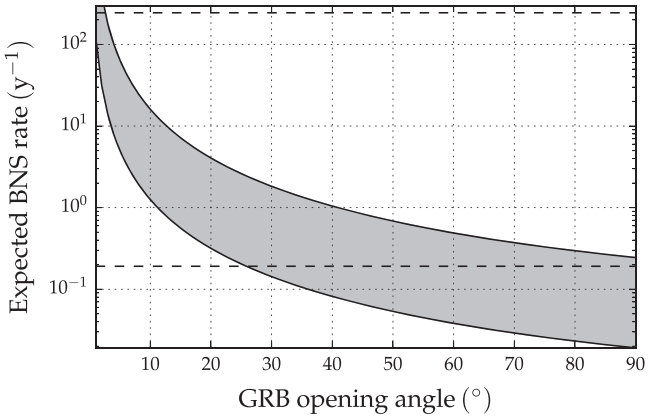

Figure 3. Expected rate of observed BNS signals when the LIGO and Virgo detectors are operating at their design sensitivity. We take the intrinsic GRB rate to be in the range 110×10^{-9} Mpc^{-3} yr^{-1}. The rate increases with smaller opening angles as this implies a greater fraction of sources which are not observed as GRBs. The horizontal lines bound the predicted number of observations based upon estimates of BNS rates. At the largest opening angles, only the higher GRB rates are consistent with the BNS predictions.

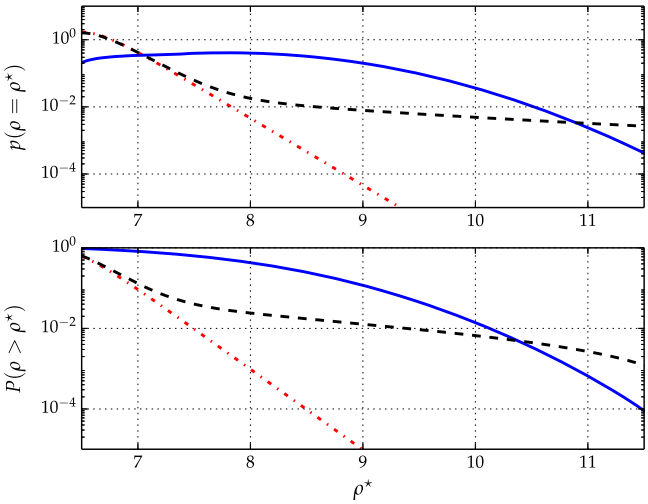

Figure 4. Probability of obtaining an event of a given SNR for: noise only (the red, dot–dashed line); a GRB progenitor at an unknown distance (the black, dashed line) and a known distance (the blue, solid line). In this example, we have used the parameters from GRB 080905A with a distance of 550 Mpc which gives a signal SNR of 7.7. The top plot shows the probability distribution function, while the bottom plot gives the cumulative probability of observing an event as loud or louder.

GRB opening angle is due to the beaming of the GW signal: the amplitude for a face on signal is a factor of 1.5 greater than the orientation averaged signal, giving a factor of 3.4 between small opening angles and no beaming. Figure 3 shows the expected all sky BNS merger rate, as a function of GRB opening angle under the assumption that *all* BNS mergers produce gamma-ray emission. As discussed in Chen & Holz (2013), there is a crossover point, where we see more GWs associated with GRBs than in an all sky, all time search. This will obviously depend upon the sky coverage and sensitivity of the GRB satellites, but assuming full sky coverage, this occurs around 40°. If the beaming angle is larger than this, the GRB search will detect more signals than the all sky all time search, due to the ability to lower thresholds around the time of observed GRBs. Of course, based on astrophysical measurements of GRB opening angles, this is unlikely to be the case.

The expected rates of short GRB observations, assuming a NSBH progenitor are given in Table 2. For NSBH mergers, the masses and spins of the system have a stronger effect upon the expected rates of observation. Higher masses and large, aligned spins result in greater GW emission increasing the distance to which the sources can be observed. For simplicity, we take the system to be a neutron star of mass $1.4M_\odot$ and a non-spinning black hole of mass $5.0M_\odot$. Following the same procedure as before, we assume that *all* GRB progenitors are NSBH binaries and use the GRB model discussed in Section 2.1 to determine the fraction of GRB signals that are observed by *Swift* and *Fermi*. This has a significant impact on the rate of observable signals, particularly in the epochs after 2019.

Table 2
The Expected Rate of Joint Gravitational Wave–GRB Observations in the Upcoming Science Runs, Assuming That the Progenitor of Every Short GRB is a NSBH Merger

Epoch	Run Duration	BNS Range (Mpc)		Number of NSBH Detections	Number of GW–GRB Detections		
		LIGO	Virgo		All Sky	*Fermi* GBM	*Swift* BAT
2015	3 months	70–130	⋯	0.0001–1	3×10^{-4}–0.06	2×10^{-4}–0.03	4×10^{-5}–0.007
2016–17	6 months	130–200	30–100	0.002–10	0.005–0.5	0.003–0.3	7×10^{-4}–0.07
2017–18	9 months	200–280	100–140	0.01–40	0.03–2	0.02–1	0.004–0.3
2019+	(per year)	330	110–220	0.05–100	0.2–6	0.1–2	0.02–0.5
2022+	(per year)	330	220	0.1–200	0.4–10	0.2–3	0.03–0.7

Note. Sensitivities and run durations taken from (Aasi et al. 2013), we assume a fiducial NSBH with a neutron star mass of $1.4M_{\odot}$ and a black hole mass of $5.0M_{\odot}$.

As we have discussed previously, there is already a tension between the observed GRB rates and predicted NSBH rates. Specifically, as is clear from Figure 1, for *all* short GRBs to have an NSBH origin requires a merger rate at the high end of the predicted range, a relatively large GRB opening angle, or both. Additionally, numerical simulations indicate that for a large fraction of NSBH mergers, there will not be sufficient matter in the accretion disk to power a GRB, making the rates even less compatible (Foucart 2012). Thus, the assumption that *all* GRBs are due to NSBH mergers seems difficult to accommodate, meaning that the highest rates in Table 2 are not realistic. Nonetheless, even if 15% of GRBs have NSBH progenitors, this would double the expected rate of joint observations. Alternatively, the absence of a joint GW–GRB observation could be used to limit the fraction of short GRBs which have a NSBH progenitor.

To end this section, we compare our results with other recently published works. Wanderman & Piran (2015) calculate the rate of joint GRB–GW detections by simply assuming a 300 Mpc range for the advanced LIGO–Virgo network. They obtain a rate of joint *Fermi* (*Swift*) observations of 0.4 ± 0.2 (0.06 ± 0.03) assuming a minimum peak luminosity of 5×10^{49} erg s^{-1}. This is entirely consistent with the rates for BNS in the 2019+ epoch given in Table 1. The fact that they have neglected the directional sensitivity of the GW network has little impact as essentially all GRBs within the advanced LIGO–Virgo range will be observable by *Swift* and *Fermi*. By varying the luminosity threshold, they obtain rates that span the same range as ours. For NSBH systems, they assume a 1 Gpc range for the advanced GW detectors, compared to our range of 660 Mpc, and consequently obtain a significantly higher rate (5 ± 2 for *Fermi* and 0.7 ± 0.3 for *Swift*). Regimbau et al. (2015) have also calculated joint detection rates of GW–GRB signals. They predict rates of joint observations with *Swift* of $0.01-0.5$ year^{-1} for BNS and $0.004-0.16$ year^{-1} for NSBH. The rates are broadly comparable to those presented here, although the range goes somewhat higher for BNS and lower for NSBH. These differences arise due to different choices of parameters in the Band function, GRB luminosity distribution, and detector thresholds. Additionally, the authors choose a fixed BNS (NSBH) rate of 6×10^{-8}(3×10^{-9}) Mpc^{-3} yr^{-1} and a range of opening angles between 5° and 30°. With these rates, NSBH signals could only account for a fraction of GRBs. This explains why their numbers are lower than the ones in Table 2 where we have assumed that *all* GRBs have NSBH progenitors.

5. BENEFITS OF JOINT OBSERVATIONS

Numerous previous papers have discussed the benefits of joint GW–GRB observations, including: the potential to confirm (or rule out) the binary merger progenitor model (Eichler et al. 1989); measuring the time-delay between the binary merber and the GRB signals to understand jet breakout; the ability to probe GRB jet opening angles (Dietz 2011; Chen & Holz 2013); the independent measurement of distance and redshift used as a probe of cosmology (Schutz 1986; Nissanke et al. 2010). We will not discuss all of these in detail, but will focus on two issues. First, we discuss how the measurement of a GRB redshift may actually assist in the detection of a GW counterpart. Then, we discuss prospects for measuring or constraining opening angles.

5.1. Detecting a GRB with Measured Redshift

The advanced detector network will, on average, be sensitive to a BNS merger associated with a GRB within a distance of 400 Mpc, or $z \lesssim 0.1$. The closest observed short GRB is GRB 080905A with a measured redshift of $z = 0.12$ (Rowlinson et al. 2010). It is interesting to ask whether this GRB could have been observed by the advanced LIGO–Virgo network. While the GRB was at a distance of 550 Mpc, it was at a favorable sky location for the advanced LIGO and Virgo network and a BNS merger associated with this GRB may have been marginally detectable, but only once the redshift information is folded in.

Let us consider the expected distribution of the observed SNR in the GW search, under three distinct scenarios: no observed GW signal; a BNS merger signal associated with a short GRB at an unknown distance; a BNS merger signal at 550 Mpc. To obtain the distribution in the absence of a signal, we simply use the empirical estimate provided in Equation (3). For a signal at 550 Mpc in the direction of GRB 080905A, a BNS merger will generate an expected network SNR of 7.7. The expected, maximum SNR observed in the GW search then follows a non-central χ^2 with four degrees of freedom (Harry & Fairhurst 2011) overlaid on the noise background given in Equation (3). Finally, for a GRB with unmeasured redshift, we use the distance distribution as given in Equation (5), i.e., signals distributed uniformly in D^3 at low redshift, with only a small probability of the GRB occurring within the LIGO–Virgo sensitive range.

In Figure 4, we show the probability distribution for the SNR of the GW event under these three scenarios. The figure shows both the probability distribution as well as the cumulative probability of observing an event above a given SNR. In this

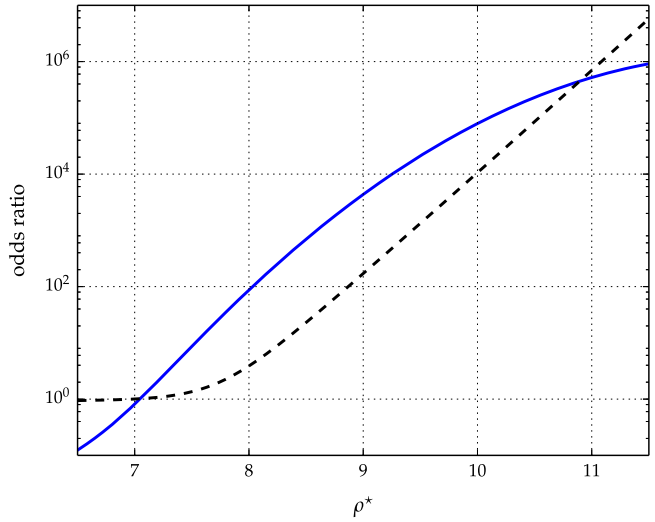

Figure 5. Odds ratio between the signal and noise models. We consider two signal models: a GRB at unknown distance (black, dashed line) and a GRB at a known distance (blue, solid line). In this example, we have used the parameters from GRB 080905A with a distance of 550 Mpc which gives an expected SNR of 7.7. The blue curve gives the odds ratio for a BNS signal at that distance, as a function of SNR. The black curve gives the odds ratio for a BNS signal at an unknown distance. At low SNR, knowledge of the distance increases the odds ratio significantly; at higher SNRs it decreases the odds as the observed SNR is no longer consistent with the distance.

example, the knowledge of the distance greatly increases the chance of observing a signal with a moderate SNR. For example, the chance of observing an event with SNR > 7.5 due to noise alone is around 1%, if there is a BNS merger at unknown distance it is 3% while when the distance is known to be 550 Mpc it is 60%.

One way to visualize the benefit of a redshift measurement is through the odds ratio: the ratio of the signal probability to the noise probability. This is plotted in Figure 5. For an observed SNR above 7.5, the signal model is favored over the noise by a factor of 10, increasing to 100 at SNR of 8. Even at these low SNRs, this would be an interesting event. However, if the distance is not known, a larger SNR (of 8.5 or 9) is required before the signal model is strongly favored over the noise. Thus, if this GRB had occurred during the advanced detector era, there is a real chance that measuring the redshift would make the difference between identifying a GW candidate and not.

5.2. Constraining the Jet Opening Angle

A joint GW–GRB observation would provide a measurement of the binary's inclination angle and, consequently, would provide a constraint on the jet opening angle of GRBs. However, the majority of observed GW signals are likely to be weak, with an SNR of ten or less, and this will make accurate parameter recovery difficult. Accurate measurement of the binary inclination angle is further complicated by the fact that it is highly degenerate with the distance, particularly when the signal is close to face on. Specifically, the overall amplitude of the two polarizations scale as $\frac{(1+\cos^2\iota)}{2D}$ and $\frac{|\cos\iota|}{D}$ and, at SNR of 10, we would expect to measure these amplitudes with roughly a 10% accuracy.

For a face on signal (with $\iota \approx 0$ or π), the two amplitudes are equal. They differ by 1% for an inclination angle of 30° and by 10% for an inclination of 50°. Thus, while the GW observation will constrain opening angles, it is most likely to limit the angle to be $\lesssim$45°. In the case where the redshift, and hence distance D, is known there will still be a ∼10% uncertainty in $\cos\iota$ corresponding to a constraint on the opening angle of $\lesssim$25°. Even for the loudest signals, we are faced with an uncertainty in the Hubble constant of 1% and a likely instrumental calibration error of 1% or more (Abadie et al. 2010a) making it difficult to constrain the opening angle to less than 10°.

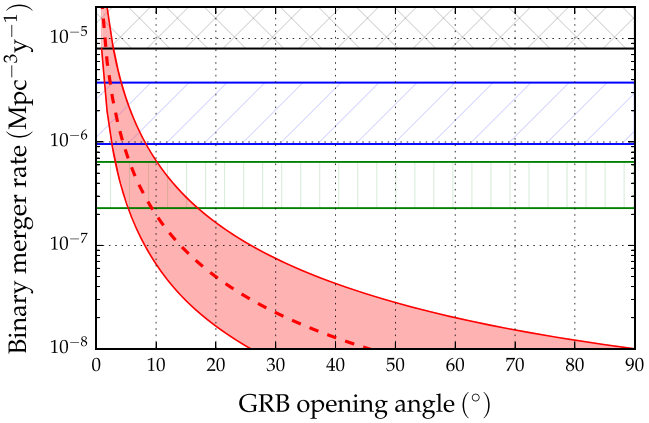

Figure 6. Expected upper limit on BNS rate for the planned observing runs, assuming that no GW events are observed: 2015 in black; 2016–17 in blue and 2017–18 in green. The ranges correspond to the uncertainties in detector sensitivity as detailed in Table 1. The expected rate of GRB progenitors as a function of the GRB opening angle is overlaid in red. Assuming that all GRBs correspond to BNS, we can read off the lower limit on opening angle that would be obtained at the end of each run.

It is more likely that the observed populations of short GRBs and binary mergers will allow us to restrict the opening angle of GRB jets. It is clear from Figure 1 how this would be done: if the permitted range of BNS merger rates can be reduced from three orders of magnitude to a factor of two, then the GRB opening angle will be highly constrained. First, consider the case where the early science runs do not yield a GW detection. We assume that, in the absence of a detection, the loudest event is consistent with background and estimate the expected rate upper limit as $R^{\rm ul} = 2.3/VT$—where V is the volume searched and T the time (Brady & Fairhurst 2008). From this, we can read off the smallest opening angle consistent with the rate upper limit by re-arranging Equation (2) to obtain

$$1 - \cos\theta \geqslant \frac{R_{\rm GRB}}{f_\gamma R^{\rm ul}_{\rm BNS}}. \quad (6)$$

Thus, the tightest limit on θ is given by assuming the maximum BNS rate, i.e., right at the upper limit, and an f_γ of unity, i.e., that all BNS mergers produce GRBs. In Figure 6 we plot the expected upper limits, in the absence of a GW detection, from the early observing runs. The bands here correspond to the uncertainties in detector sensitivities as given in Figure 1. For example, at the end of the 2016–17 run, the lack of a detection can place a constraint on the GRB opening angle between 2° and 8° depending upon the detector sensitivity achieved and the assumed GRB rate. Thus, even in the absence of an observation, we are starting to impact measurements from GRB observations. In Table 3, we summarize the results for BNS signals, and also for NSBH. In both cases, we are

Table 3
The Expected Bounds on GRB Opening Angle During the Early Advanced LIGO–Virgo Observing Runs

Epoch	Run Duration	BNS Range (Mpc)		Limit on GRB Opening Angle (°)	
		LIGO	Virgo	BNS	NSBH
2015	3 months	40–80	⋯	0–3	0–6
2016–17	6 months	80–120	20–60	1–8	3–15
2017–18	9 months	120–170	60–85	3–15	7–35

Notes. These results assume that no gravitational wave signal is observed and use the observed GRB rate to infer the minimum jet opening angle consistent with the lack of gravitational wave detection. The results in the two columns assume that all GRBs are either BNS (first column) or NSBH (second). In both cases, the range quoted takes into account both the uncertainty in the detector performance in these runs as well as the uncertainty in the local rate of GRBs.

assuming that all GRBs are produced by one particular type of merger. This, of course, is unrealistic. Although we cannot know the fraction of GRBs which have a BNS or NSBH progenitor, we might reasonably assume that *all* GRB progenitors are mergers. Since the sensitivity to BNS mergers is less than NSBH, the conservative limit comes from assuming that all mergers are BNS. Alternatively, it is possible to make reasonable assumptions of priors for the various parameters and then marginalize over them to obtain a distribution for the opening angle (J. Clark et al. 2014, in preparation).

Of course, we hope to observe GWs from binary mergers. Even a handful of observations will provide a measurement of the rate within a factor of two, which will correspond to a much tighter horizontal band on Figure 1. If, for example, the rate is 10^{-6} Mpc^{-3} yr^{-1} then this will restrict the GRB opening angle to be between about 3° and 8°.

6. CONCLUSION

We have presented in detail the expectations for GW observations associated with short GRBs in the coming years. The evidence for a binary merger progenitor of short GRBs is strong, and we have focused on this scenario. By making use of the known time and sky location of the source, we have argued that it is appropriate to lower the GW search threshold by around 25% relative to the all sky, all time search. This decrease in threshold will double the number of GW events that can be detected in association with a GRB. We have also demonstrated that if the redshift is measured (and is within the sensitive range of GW network), the detection threshold can be further reduced. Using this threshold reduction and the expected evolution of GW detector sensitivities given in Aasi et al. (2013), a joint GW–GRB observation is possible in the 2015 and 2016–17 observing runs, but unlikely. However, as the detectors approach their design sensitivity the rate of joint observations increases and could be one or two per year for a BNS progenitor and even higher if the majority of GRBs have NSBH progenitor. This, of course, depends critically upon the continued operation of wide-field of view GRB satellites, such as *Fermi*, as well as the continued operation of the IPN.

The joint observation of GW and GRB signals will be a major milestone in understanding short GRBs, and will finally prove (or disprove) the binary merger progenitor scenario. It will also shed light on the GRB central engine by probing delays between the signals and a bound on the jet opening angle. We have argued that the measurement of binary inclination from GW observations will have large uncertainties, due in part to the degeneracy with the measurement of distance, and is unlikely to constrain the opening angle tightly. However, an accurate measurement of the populations of both short GRBs and BNS (or NSBH) mergers will allow us to constrain the opening angle. Even in the early advanced detector runs, we will be able to place lower bounds on the beaming angle of short GRBs that will confront current observations.

The authors would like to thank the participants of the Royal Society International Scientific Seminar on Gravitational Waves and Gamma-Ray Bursts for useful discussions. In addition, they thank Ray Frey and Valeriu Predoi for comments on the manuscript. This work was supported by the UK Science and Technologies Funding Council through grant ST/L000962/1, the Royal Society and the US National Science foundation through grants PHY-0847611, PHY-1205835, PHY-0955773, and AST-1333142.

REFERENCES

Aasi, J., Abadie, J., Abbott, B. P., et al. 2013, arXiv:1304.0670
Aasi, J., Abadie, J., Abbott, B. P., et al. 2014, PhRvL, 113, 011102
Aasi, J., Abbott, B. P., Abbott, T., et al. 2015, CQGra, 32, 074001
Abadie, J., Abbott, B. P., Abbott, R., et al. 2010a, NIMPA, 624, 223
Abadie, J., Abbott, B. P., Abbott, R., et al. 2010b, CQGra, 27, 173001
Abadie, J., Abbott, B. P., Abbott, R., et al. 2012b, ApJ, 760, 12
Abadie, J., Abbott, B. P., Abbott, R., et al. 2012c, PhRv, D85, 082002
Abadie, J., Abbott, B. P., Abbott, T. D., et al. 2012a, ApJ, 755, 2
Abbott, B., Abbott, R., Adhikari, R., et al. 2008, ApJ, 681, 1419
Abbott, B. P., Abbott, R., Adhikari, R., et al. 2009, RPPh, 72, 076901
Acernese, F., Amico, P., Alshourbagy, M., et al. 2007, CQGra, 24, S381
Acernese, F., Adams, T., Agathos, M., et al. 2015, JPhCS, 610, 012014
Allen, B. 2005, PhRvD, 71, 062001
Babak, S., Biswas, R., Brady, P. R., et al. 2013, PhRv, D87, 024033
Band, D., Matteson, J., Ford, L., et al. 1993, ApJ, 413, 281
Basa, S., Wei, J., Paul, J., & Zhang, S. 2008, arXiv:0811.1154
Berger, E. 2014, ARA&A, 52, 43
Berger, E., Fong, W., & Chornock, R. 2013, ApJL, 774, L23
Blanchet, L. 2014, LRR, 17,
Bloom, J. S., Djorgovski, S., Kulkarni, S., & Frail, D. 1998, ApJL, 507, L25
Brady, P. R., & Fairhurst, S. 2008, CQGra, 25, 105002
Bromberg, O., Nakar, E., Piran, T., & Sari, R. 2013, ApJ, 764, 179
Chen, H.-Y., & Holz, D. E. 2013, PhRvL, 111, 181101
Coward, D. M., Howell, E. J., Piran, T., et al. 2012, MNRAS, 425, 2668
Dietz, A. 2011, A&A, 529, A97
Dietz, A., Fotopoulos, N., Singer, L., & Cutler, C. 2013, PhRv, D87, 064033
Dominik, M., Belczynski, K., Fryer, C., et al. 2012, ApJ, 759, 52
Eichler, D., Livio, M., Piran, T., & Schramm, D. N. 1989, Natur, 340, 126
Fong, W., Berger, E., Metzger, B. D., et al. 2014, ApJ, 780, 118
Fong, W.-F., & Berger, E. 2013, ApJ, 776, 18
Foucart, F. 2012, PhRvD, 86, 124007
Gehrels, N., Barbier, L., Barthelmy, S., et al. 2005, Natur, 437, 851
Gehrels, N., Chincarini, G., Giommi, P., et al. 2004, ApJ, 611, 1005
Giacomazzo, B., Rezzolla, L., & Troja, E. 2012, ApJL, 762, L18
Guelbenzu, A. N., Klose, S., Greiner, J., et al. 2012, A&A, 548, A101
Guetta, D., & Piran, T. 2006, A&A, 453, 823
Harry, I. W., & Fairhurst, S. 2011, PhRv, D83, 084002
Hjorth, J., Sollerman, J., Moller, P., et al. 2003, Natur, 423, 847
Hjorth, J., Watson, D., Fynbo, J. P., et al. 2005, Natur, 437, 859
Hurley, K., Cline, T., Mitrofanov, I., et al. 2003, in AIP Conf. Proc. 662, Gamma-Ray Burst and Afterglow Astronomy 2001: A Workshop Celebrating the First Year of the HETE Mission, 473
Hurley, K., Goldsten, J., Golenetskii, S., et al. 2007, GCN, 6103, 1
Hurley, K., Rowlinson, A., Bellm, E., et al. 2010, MNRAS, 403, 342
Kelley, L. Z., Mandel, I., & Ramirez-Ruiz, E. 2013, PhRv, D87, 123004
Klebesadel, R. W., Strong, I. B., & Olson, R. A. 1973, ApJL, 182, L85
Kouveliotou, C., Meegan, C. A., Fishman, G. J., et al. 1993, ApJL, 413, L101

Meegan, C., Lichti, G., Bhat, P., et al. 2009, ApJ, 702, 791
Nakar, E. 2007, PhR, 442, 166
Nissanke, S., Holz, D. E., Hughes, S. A., Dalal, N., & Sievers, J. L. 2010, ApJ, 725, 496
Owen, B. J., & Sathyaprakash, B. S. 1999, PhRv, D60, 022002
Panaitescu, A. 2006, MNRAS Lett., 367, L42
Pannarale, F., & Ohme, F. 2014, ApJL, 791, L7
Piran, T., Nakar, E., & Rosswog, S. 2013, MNRAS, 430, 2121
Predoi, V., & Hurley, K. 2012, JPhCS, 363, 012034
Regimbau, T., Siellez, K., Meacher, D., Gendre, B., & Bor, M. 2015, ApJ, 799, 69
Rowlinson, A., Wiersema, K., Levan, A. J., et al. 2010, MNRAS, 408, 383
Sari, R., Piran, T., & Halpern, J. 1999, ApJL, 519, L17
Schutz, B. F. 1986, Natur, 323, 310
Siellez, K., Boër, M., & Gendre, B. 2014, MNRAS, 437, 649
Stone, N., Loeb, A., & Berger, E. 2013, PhRv, D87, 084053
Tanvir, N. R., Levan, A. J., Fruchter, A. S., et al. 2013, Natur, 500, 547
Thorne, K. S. 1987, in Three Hundred Years of Gravitation, ed. S. W. Hawking & W. Israel (Cambridge: Cambridge Univ. Press), 330
von Kienlin, A., Meegan, C. A., Paciesas, W. S., et al. 2014, ApJS, 211, 13
Wanderman, D., & Piran, T. 2015, MNRAS, 448, 3026
Williamson, A., Biwer, C., Fairhurst, S., et al. 2014, PhRv, D90, 122004